Immunological, structural, and preliminary X-ray diffraction characterizations of the fusion core of the SARS-coronavirus spike protein ☆

Chun-Hua Hsu[1], Tzu-Ping Ko, Hui-Ming Yu, Tswen-Kei Tang, Shui-Tsung Chen, Andrew H.-J. Wang*

Institute of Biological Chemistry, Academia Sinica, Taipei 115, Taiwan, ROC

Abstract

The SARS-CoV spike protein, a glycoprotein essential for viral entry, is a primary target for vaccine and drug development. Two peptides denoted HR-N(SN50) and HR-C(SC40), corresponding to the Leu/Ile/Val-rich heptad-repeat regions from the N-terminal and C-terminal segments of the SARS-CoV spike S2 sequence, respectively, were synthesized and predicted to form trimeric assembly of hairpin-like structures. The polyclonal antibodies produced by recombinant S2 protein were tested for antigenicity of the two heptad repeats. We report here the first crystallographic study of the SARS spike HR-N/HR-C complex. The crystal belongs to the triclinic space group P1 and the data-set collected to 2.98 Å resolution showed noncrystallographic pseudo-222 and 3-fold symmetries. Based on these data, comparative modeling of the SARS-CoV fusion core was performed. The immunological and structural information presented herein may provide a more detailed understanding of the viral fusion mechanism as well as the development of effective therapy against SARS-CoV infection.
© 2004 Elsevier Inc. All rights reserved.

Keywords: SARS; Spike; Heptad repeat; Coiled coil; Pseudo-symmetry; Synchrotron radiation

Severe acute respiratory syndrome (SARS) is a severe and readily transmissible new disease that first emerged in Southern China in late 2002 and quickly spread worldwide after March 2003 [1]. The causative agent of SARS was identified to be a previously unknown member of the Coronaviridae family and named SARS-associated coronavirus (SARS-CoV) [2,3]. A safe and effective SARS-CoV vaccine is not yet available and therefore it is important to pursue potential therapeutic measures against SARS-CoV infection.

The spike (S) proteins of coronaviruses are large type-I transmembrane glycoproteins that are responsible for receptor binding and membrane fusion. Two functional domains at the amino and carboxy termini of the S protein (S1 and S2, respectively) are conserved among the coronaviruses. As shown in Fig. 1, the transmembrane segment is close to the C terminus of the S2 subunit. Adjacent to both the fusion peptide-like region and transmembrane segments are two regions containing 4,3-hydrophobic heptad repeats (HR), a sequence
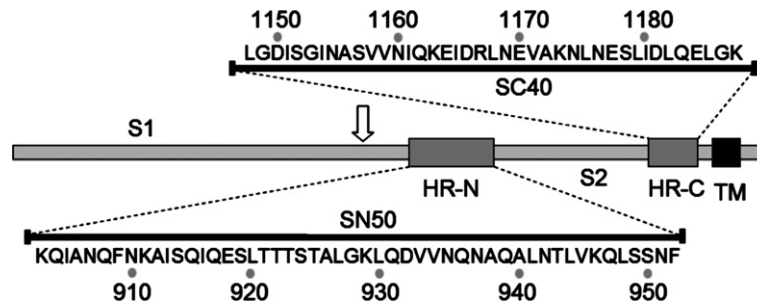
Fig. 1. Interacting peptides predicted in SARS-CoV spike protein. A schematic view of spike shows the 4–3 hydrophobic repeat (HR) and the transmembrane region (TM). The ectodomain is drawn approximately to scale. The peptides predicted by protein dissection are shown, along with the sequences of N50 (HR-N) and C40 (HR-C). The residues are numbered according to their position in the SARS-CoV spike protein sequence.

motif suggestive of coiled-coil structures [4]. These regions are denoted HR-N and HR-C, respectively, and are separated by an intervening domain of ~200 residues. The S1 and S2 domain of SARS-CoV S protein can be identified by sequence alignment with other coronavirus S proteins, especially with the more conserved S2 domain [5,6]. These coiled-coil regions are thought to play an important role in defining the oligomeric structure of the spike protein in its native state and its fusogenic ability [7].

While there is a pressing need for effective antiviral therapies against SARS, structural study of the HR regions within the ectodomain of the SARS-CoV S glycoprotein would prove to be a convenient means in the design of peptide mimics for inhibition of virus entry. A large body of evidence suggests that fusion mediated by several type 1 viral fusion proteins, e.g., HIV-1, can be inhibited by peptide mimics of the HR-N or HR-C regions [8,9]. To obtain the 3D-structural information, crystallization of the HR-N/HR-C complex of SARS-CoV spike protein has been carried out. In addition, immunological characterization of the heptad repeats of the spike protein was performed. We report here the first crystal and preliminary X-ray analysis of the SARS spike HR-N/HR-C complex.

Materials and methods

Molecular cloning and protein expression of the spike S2 protein. The DNA sequences coding the spike protein of SARS-CoV were obtained from the College of Medicine, National Taiwan University (GenBank Accession No. AY291451). The coding sequence of S2 (aa 902–1255) was amplified by PCR with primers containing 5′- and 3′-restriction sites. The PCR product was digested and ligated into the *Nde*I and *Xho*I sites of the pET-21b vector (Novagen, Madison, WI), and the construct was transformed into *Escherichia coli* strain BL21 (DE3) (Novagen, Madison, WI) for protein expression.

The recombinant S2 protein was expressed by induction with 0.5 mM isopropyl-β-D-thiogalactopyranoside for 3 h at 37 °C. The inclusion bodies were collected after the cells were broken by microfluidizer and dissolved in 8 M guanidine–HCl at room temperature for overnight. After purification using Ni–NTA affinity chromatography, the protein was then sequentially diluted in 8, 6, 4, and 2 M urea,

respectively. The protein purity was determined by 12.5% SDS–PAGE electrophoresis and visualized with Coomassie blue staining.

Peptide synthesis and purification. Peptides SN50 (HR-N) and SC40 (HR-C), having an acetylated N terminus and a C-terminal amide, were synthesized by standard FMOC peptide chemistry. SN50 corresponds to residues 903–952 of SARS-CoV spike protein, while SC40 corresponds to residues 1148–1187. After cleavage from the resin, the peptides were desalted on a Sephadex G-25 column (Pharmacia) and lyophilized. Peptides were then purified by reverse-phase high performance liquid chromatography on a Vydac C18 preparative column (Waters). The identity of the HR-N and HR-C peptides was verified by mass spectrometric analysis, with molecular weights of 5490.1 and 4405.9, respectively.

Polyclonal antibody preparation and immunodetection assays. The soluble recombinant S2 protein in 2 M urea was used as antigen for immunization and immunoassays. The New Zealand White Rabbits, weighing 300–350 μg, were immunized by intrasplenic injection with the recombinant SARS S2 protein at 250 μg per immunization. The antigen in 0.5 ml PBS was emulsified with an equal volume of Titer Max adjuvant (CytRx, Norcross, GA). The rabbit antisera were used for most of the subsequent experiments without purification. We analyzed the titer of rabbit sera using Western blot assay for S2 protein antigen. In general, we could obtain high titer polyclonal antibodies after 6–8 weeks of immunization.

The dot blot assays for synthetic HR-N and HR-C peptides were then tested using the well-prepared antisera. Synthetic HR-N (SN50), HR-C (SC40), and HR-N/HR-C were dropped onto a PVDF membrane, which was then blocked with skim milk and incubated for 16 h at 4 °C with anti-S2 rabbit antisera diluted 1:2000–3000. Bound antibodies were detected by use of horseradish peroxidase-labeled donkey anti-rabbit antibodies (Amersham Biosciences). The target peptides were revealed by an enhanced chemiluminescence (ECL, Amersham Biosciences) development system.

Circular dichroism spectroscopy. Circular dichroism (CD) spectra were measured on the Aviv CD 202 spectrophotometer in PBS buffer. Wavelength spectra were recorded from 260 to 180 nm at 25 °C using a 0.1 cm path-length cuvette. For thermodynamic stability, the HR-N/HR-C complex protein was measured at 222 nm by monitoring the CD signal in the temperature ranging from 25 to 100 °C with a scan rate of 2 °C per minute. The spectra were corrected by the subtraction of a blank corresponding to the solvent and the midpoint of the thermal unfolding transition (T_m) values was evaluated.

Native PAGE. Equimolar mixtures of the HR-N and HR-C peptides (each 0.6 mM) were dissolved in PBS buffer (pH 7.2). The samples were prepared with HR-N and HR-C alone as well as HR-N/HR-C (1:10) and HR-N/HR-C (1:1) in a total volume of 30 μl. HR-N/HR-C mixtures were incubated at room temperature for 10 min. After the addition of an equal volume of 5× N-tris(hydroxymethyl)methylglycine (Tricine) sample buffer (0.125 M Tris–HCl, pH 6.8, 10% glycerol, and 0.004 g bromophenol blue) the mixture

was analyzed by PAGE on 4–12% gradient Tricine gel with a Tricine/glycine running buffer (pH 8.3).

Crystallization. A 10 mg/ml stock solution of the HR-N/HR-C complex was prepared by dissolving the peptides with equal molar ratio in 10 mM Tris–HCl, pH 8.0. Initial crystallization screening was performed using Hampton Research Crystal Screens (Laguna Niguel, CA, USA) with the hanging-drop vapor-diffusion method. Crystallization drops were set up using the stock solution mixed with various reservoir solutions (1:1) and allowed to equilibrate at 300 K against the same reservoir in a 24-well plate.

Data collection and analysis. Preliminary X-ray diffraction experiments were carried out at cryogenic temperatures with an R-Axis IV[++] image-plate detector (Molecular Structure, The Woodlands, TX, USA) using CuKα radiation generated by a Rigaku MicroMax007 rotating-anode generator. Higher resolution data were collected using synchrotron radiation and an ADSC Quantum 4 CCD camera at BL12B2 Taiwan beam line at SPring-8, Japan. Data were processed using the software package of HKL.

Molecular modeling. The sequences of two heptad regions between SARS-CoV and MHV were aligned by using the multiple sequence alignment program, CLUSTAL W. The sequences have 56% and 28% identity (66% and 54% similarity) in the aligned HR-N and HR-C regions, respectively. The 3D models of SARS-CoV HR-N and HR-C regions of Spike protein were generated with the MODELLER program [10] encoded in InsightII (Accelrys) using MHV fusion core (PDB code: 1WDF) as the template structure. The HR-N/HR-C was assembled into the six helix bundle according the MHV fusion core structure. The model of SARS-CoV fusion core was optimized with rigid peptide backbone and 1000 steps of conjugate gradient optimization were used for energy minimization.

Several structural analysis softwares were adopted to check the model quality. The distribution of the backbone dihedral angles of the model was evaluated by the representation of Ramachandran plot using PROCHECK [11]. The PROSTAT module of InsightII was used to analyze the properties of bonds, angles, and torsions. Profile-3D program [12] was used to check the structure and sequence compatibility.

Results

HR-N and HR-C form a helical complex

The HR-N and HR-C peptides were synthesized using Fmoc chemistry. After purification using RP-HPLC, the CD experiments were carried out for these peptides and their complex. Either HR-N or HR-C peptide alone contains low α-helical characters (data not shown). Equimolar mixtures of HR-N and HR-C peptides (100 μM each) were incubated at room temperature for 3 h, to facilitate the HR-N/HR-C complex formation. After incubation, the CD spectroscopic profile of the HR-N/HR-C complex shows a typical α-helix structure with double minima at 208 and 222 nm (Fig. 2). Regarding the thermal stability, the HR-N and HR-C mixture exhibited the formation of a very stable complex. The melting temperature (T_m value) of HR-N/HR-C complex is higher than 80 °C (Fig. 2, inset). The CD spectra of the refolded HR-N/HR-C complex were also recorded after the heat-denaturation experiment. The helical contents of these peptides and complex were estimated as the following
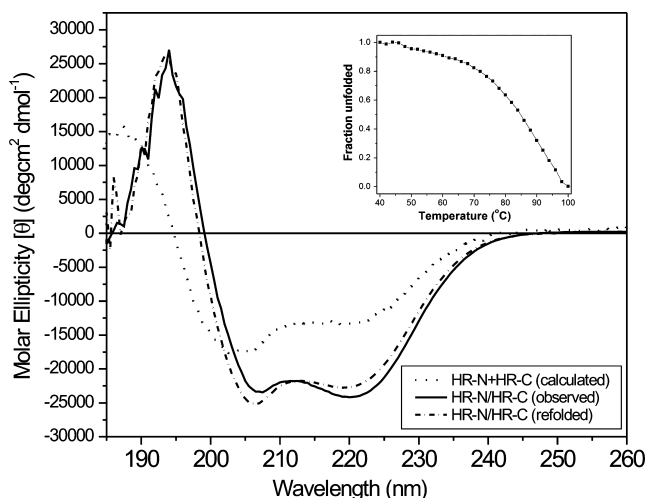

Fig. 2. Analysis of secondary structures of the HR-N + HR-C mixture and HR-N/HR-C complex in phosphate buffer. Circular dichroism spectra are presented for HR-N + HR-C mixture (calculated), and their complex in phosphate buffer (pH 7.0) at 25 °C. Inset: circular dichroism signal at 222 nm for the HR-N/HR-C complex as a function of temperature.

average percentage by the CDPro program [13]: 29.7% for HR-N + HR-C (calculated); 62.4% for HR-N/HR-C (observed); and 56.5% for HR-N/HR-C (refolded). These results show that the HR-N/HR-C complex contains a substantially higher α-helical character than the sum of HR-N and HR-C alone.

In the gel-shift experiment, the formation of HR-N/HR-C could be observed on the native gradient gel to compare with the HR-N and HR-C alone (Fig. 2A). The combination of equimolar amounts of HR-N and HR-C gives rise to the disappearance of the individual bands and the formation of new bands at the intermediate positions corresponding to the complex. Additionally, complex formation was also observed with the HR-N/HR-C (1:10) but without complete disappearance of the individual HR-C component. Therefore, the two sets of data, CD and PAGE, strongly suggest that HR-N/HR-C form a stable helical complex derived from the key region of interaction and agree with the previous reports of the post-fusion states of type-I viral protein fusion core. Some interesting phenomenon was observed on the native PAGE gel. Beside the major bands, smearing bands appear in the lanes of either HR-C or HR-N/HR-C which may be caused by the equilibrium between the ordered and disordered HR-C peptides. Furthermore, the various combinations of HR-N and HR-C (HR-N homotrimer, HR-N/HR-C heterodimer, trimer of the HR-N/HR-C heterodimer, and HR-N/HR-C complex with dynamic equilibrium of HR-C release) could form several major bands on the native 4–12% gradient gel (Fig. 3A).
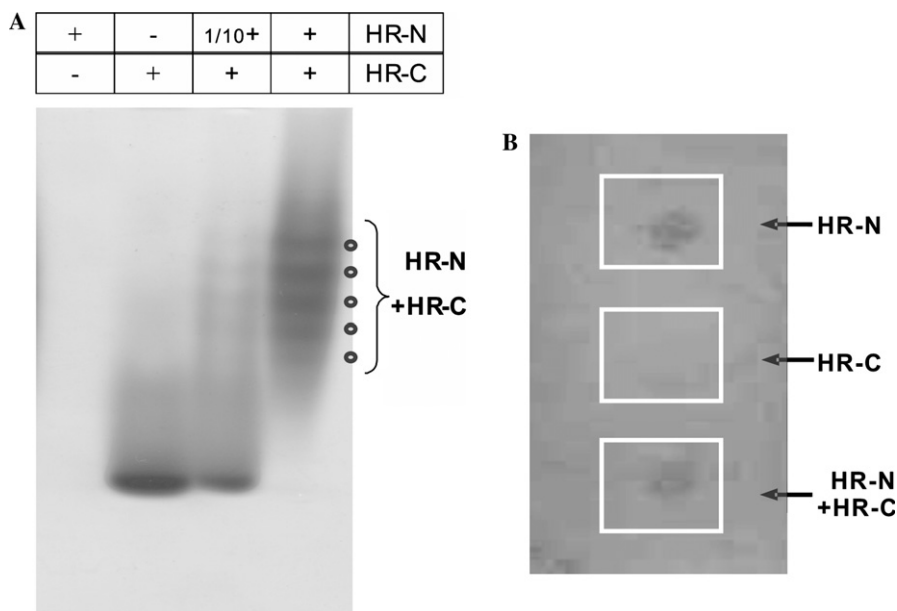
Fig. 3. (A) Analysis of the interaction of HR-N and HR-C peptides by native PAGE. HR-N peptide alone is not visible because it is positively charged (pI = 9.53) under the gel electrophoresis condition (buffer pH 8.3 and the positive-charge electrode on the bottom). By contrast, HR-C (pI = 4.44) and HR-N/HR-C complex (pI = 5.22) are negatively charged and observed on the native PAGE gel. The HR-N and HR-C mixture at molar ratio 1:10 on the gel reveals the decrease of HR-C band and the formation of HR-N/HR-C complex. (B) Dot blotting immunoassay of HR-N and HR-C peptides shows the higher antigenicity of HR-N region.

Crystallization and X-ray diffraction analysis of the HR-N/HR-C complex

After the optimization of crystallization conditions, crystals of HR-N/HR-C (SN50/SC40) complex were grown using a reservoir solution containing 100 mM Na–Hepes, pH 7.5, 20% PEG4000, and 10% isopropanol. Prior to data collection, crystals were mounted in a cryoloop and the reservoir solution with addition of 5% PEG200 was used as a cryoprotectant. Initially, due to the fact that the unit cell is nearly orthorhombic, attempts were made to process the data sets by the space group of P222 and P2. However, the results were not acceptable. Finally, the crystals were determined to belong to the triclinic space group P1 with unit-cell parameters $a = 50.99$ Å, $b = 58.40$ Å, $c = 76.03$ Å, and $\alpha = 90.52°$, $\beta = 89.99°$, $\alpha = 89.98°$ as well as unit-cell volume of 226,382 Å^3. The data were collected to 2.98 Å resolution with the statistics as the following: 36,316 for number of observations; 28,326 for unique reflections; 94.7% for completeness; 8.7% for R_{merge}; and 10.6 I for average I/σ. The self-rotation function maps revealed three perpendicular 2-fold axes and a 3-fold axis (data not shown). These non-crystallographic symmetries suggest that the SN50/SC40 complex forms three-helical bundles whose long axis is approximately parallel to the crystallographic c-axis, and there are probably four such trimeric assemblies in an asymmetric unit related by pseudo-222 symmetry. This prediction is further justified by calculating the Matthews coefficient V_{m} [14], which is 1.91 Å^3/Da by assuming 4 timers of HR-N/HR-C in an asymmetric unit with a solvent content of about 35%.

Immunization of recombinant S2 protein and immunoassays of synthetic heptad peptides

The S protein is the major antigen determinant site and the viral protein responsible for the recognition by host cells. The N-terminus of the S protein (S1) contains the receptor-binding domain (RBD) for the host cell recognition. Angiotensin-converting enzyme 2 (ACE2) was identified as the functional receptor for the SARS coronavirus [15] and the binding site of spike protein has been mapped to 193 amino-acid fragment (aa 318–510) of the S1 region [16]. The S2 region including two heptad repeats is associated with the fusion mechanism of virus entry. We expressed recombinant S2 protein (aa 902–1255) for the antibody production. Once the antisera were generated, the dot blotting immunoassay was carried out with the anti-S2 antibodies (Fig. 3B). The result revealed that the anti-S2 antibodies could recognize HR-N better than HR-C, suggesting a greater immunogenicity for the HR-N region. Thus, HR-N is the better target for vaccine development. On the other hand, the low-immunogenic HR-C region could be used as the peptide drug to block virus entry.

Molecular modeling of SARS spike fusion core

Recently, the crystal structure of mouse hepatitis virus (MHV) spike fusion core has been reported [17]. Alignments of the HR-N and HR-C peptides on the corresponding MHV spike N-peptides and C-peptides revealed reasonable sequence similarities. Thus, we could confidently build a homology model of the HR-N and HR-C association based on the X-ray crystal structure of the MHV spike core formed between the N-peptides and C-peptides. HR-N peptides possessed a typical triple coiled-coil structure as shown by the red ribbons in Fig. 4B. Half of HR-C (blue ribbons) had an α-helical conformation with the exception of an extended coil in the middle of the structure. Surface map representation shows the presence of the hydrophobic grooves on the surface of three central HR-N helices. Three HR-C helices pack against the hydrophobic groove in an anti-parallel manner. The extended coil region packs against the shallow groove, but the helical region of HR-C packs against the deep groove (Fig. 4C). The sequences between SARS-CoV and MHV share 66% and 54% similarity (56% and 28% identity) in the aligned HR-N and HR-C regions, respectively. The residues at the "a" and "d" positions in the HR-N and HR-C regions are hydrophobic (Fig. 4A). The complex structure derived from superimposing with the MHV crystal structure also shows that there are hydrophobic interactions between these two peptides (Fig. 4C). Before the

crystal structure of SARS spike fusion core is solved, this homology model could be used as the guide for searching the inhibitory ligands through virtual docking screen technique.

Discussion

Fusion of the virus envelope with cellular membrane is a prerequisite for viral entry into target cells, and thus a critical step in the life cycle of all enveloped viruses. The fusion mechanism has been well studied and revealed that the HR-N/HR-C six helix bundle formation is important for the viral entry [4]. If small, oral, bioavailable molecules that disrupt the formation of HR-N/HR-C complex could be identified, they may be developed into effective drugs against viral infection. The first goal of this project was to solve the HR-N/HR-C complex structure. The 3D structure of the spike fusion core will be helpful for rational drug design or virtual screening by docking program in anti-SARS therapy.

We produced the S2 antibody to detect the immunogenicity of HR-N and HR-C. Interestingly, the immunogenicity of HR-N is greater than that of HR-C. According to the result, the peptide corresponding to the HR-C region seems to be a better candidate for disrupting the formation of six-helix bundle, since it is less likely to be serum neutralized than HR-N peptide. On the other hand, HR-N is the better candidate of
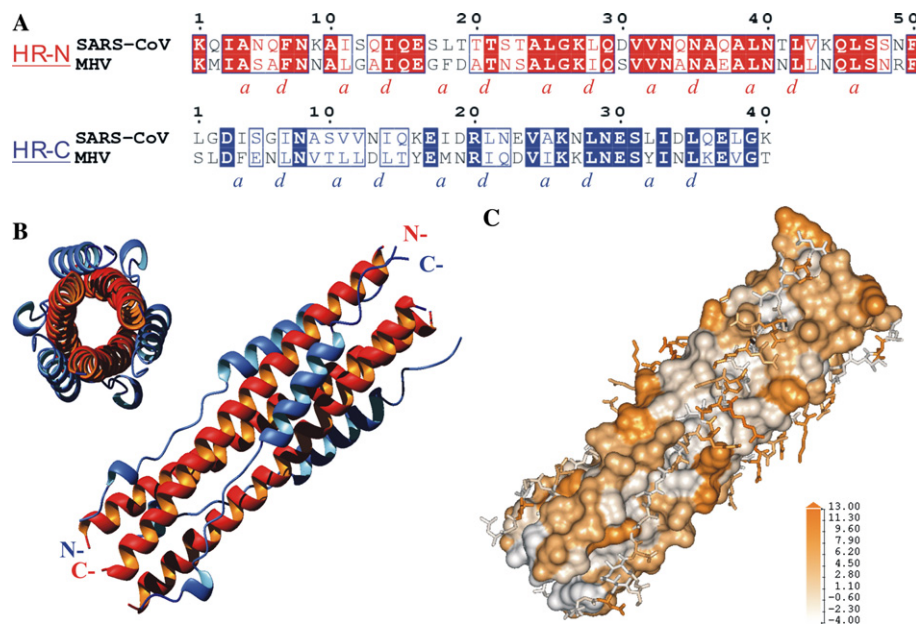

Fig. 4. Homology modeling of SARS-CoV fusion core. (A) Pairwise sequence alignments of HR-N (top) and HR-C (bottom) regions between SARS-CoV and MHV. (B) 3D Model of SARS-CoV fusion core is presented as six-helix bundle (trimer of heterodimers) by side view (right). The 3-fold axis of the HR-N trimer is shown as top view (left). HR-N and HR-C are colored with red and blue, respectively. (C) Representation of the HR-N coiled coil as a molecular surface, with the three HR-C helices depicted as sticks. The HR-C helices pack against a conserved groove on the surface of the coiled coil in the antiparallel manner. The triple coiled coil of HR-N has some large cavity that provides the hydrophobic binding pocket for the hydrophobic residues of three HR-C peptides. The colors of surface and stick are painted with orange to white gradient from hydrophobic to hydrophilic properties.

anti-SARS vaccine than the HR-C region, since the former has higher antigenicity.

Several structures of enveloped viral fusion protein cores have been determined thus far [4]. The four viral families with the most extensive structural information are orthomyxovirus, retrovirus, paramyxovirus, and filovirus. During the course of our project, the structure of MHV fusion protein core in the coronavirus family was reported [17]. Molecular replacement searches were carried out with models from MHV fusion core (PDB code: 1WDF) and other viral families, including the crystal structure of paramyxovirus SV5 fusion protein core (PDB code: 1SVF) [18] and human respiratory syncytial virus (HRSV) fusion protein core (PDB code: 1G5C) [19]. Cross rotation function searches yielded a series of peaks that are consistent with the self-rotation function results, i.e., most of the α-helices are nearly parallel to the crystallographic *c*-axis.

We are currently working on heavy atom derivatives and trying to solve the structure using the MIR or MIRAS methods. In addition, we are preparing other HR-N and HR-C peptides with different lengths and searching for new crystallization conditions to obtain new crystals in different space groups, hopefully with fewer molecules in the unit cell, to facilitate structure determination by molecular replacement.

In conclusion, we report here the first crystal and preliminary X-ray analysis of the SARS spike HR-N/HR-C complex. In addition, the comparative modeling is applied to build the homology model of SARS-CoV fusion core. On the basis of the model, we could further design the suitable peptide derivatives for solving the crystal phase and peptide analogs for efficient inhibition of virus entry. The docking experiments of the SARS-CoV fusion core model are also being carried out for virtual screening of anti-virus drugs.

Acknowledgments

References

[1] J.S. Peiris, C.M. Chu, V.C. Cheng, K.S. Chan, I.F. Hung, L.L. Poon, K.I. Law, B.S. Tang, T.Y. Hon, C.S. Chan, K.H. Chan, J.S. Ng, B.J. Zheng, W.L. Ng, R.W. Lai, Y. Guan, K.Y. Yuen, Clinical progression and viral load in a community outbreak of coronavirus-associated SARS pneumonia: a prospective study, Lancet 361 (2003) 1767–1772.

[2] C. Drosten, S. Gunther, W. Preiser, S. van der Werf, H.R. Brodt, S. Becker, H. Rabenau, M. Panning, L. Kolesnikova, R.A. Fouchier, A. Berger, A.M. Burguiere, J. Cinatl, M. Eickmann, N. Escriou, K. Grywna, S. Kramme, J.C. Manuguerra, S. Muller, V. Rickerts, M. Sturmer, S. Vieth, H.D. Klenk, A.D. Osterhaus, H. Schmitz, H.W. Doerr, Identification of a novel coronavirus in patients with severe acute respiratory syndrome, N. Engl. J. Med. 348 (2003) 1967–1976.

[3] T.G. Ksiazek, D. Erdman, C.S. Goldsmith, S.R. Zaki, T. Peret, S. Emery, S. Tong, C. Urbani, J.A. Comer, W. Lim, P.E. Rollin, S.F. Dowell, A.E. Ling, C.D. Humphrey, W.J. Shieh, J. Guarner, C.D. Paddock, P. Rota, B. Fields, J. DeRisi, J.Y. Yang, N. Cox, J.M. Hughes, J.W. LeDuc, W.J. Bellini, L.J. Anderson, A novel coronavirus associated with severe acute respiratory syndrome, N. Engl. J. Med. 348 (2003) 1953–1966.

[4] D.M. Eckert, P.S. Kim, Mechanisms of viral membrane fusion and its inhibition, Annu. Rev. Biochem. 70 (2001) 777–810.

[5] M.A. Marra, S.J. Jones, C.R. Astell, R.A. Holt, A. Brooks-Wilson, Y.S. Butterfield, J. Khattra, J.K. Asano, S.A. Barber, S.Y. Chan, A. Cloutier, S.M. Coughlin, D. Freeman, N. Girn, O.L. Griffith, S.R. Leach, M. Mayo, H. McDonald, S.B. Montgomery, P.K. Pandoh, A.S. Petrescu, A.G. Robertson, J.E. Schein, A. Siddiqui, D.E. Smailus, J.M. Stott, G.S. Yang, F. Plummer, A. Andonov, H. Artsob, N. Bastien, K. Bernard, T.F. Booth, D. Bowness, M. Czub, M. Drebot, L. Fernando, R. Flick, M. Garbutt, M. Gray, A. Grolla, S. Jones, H. Feldmann, A. Meyers, A. Kabani, Y. Li, S. Normand, U. Stroher, G.A. Tipples, S. Tyler, R. Vogrig, D. Ward, B. Watson, R.C. Brunham, M. Krajden, M. Petric, D.M. Skowronski, C. Upton, R.L. Roper, The Genome sequence of the SARS-associated coronavirus, Science 300 (2003) 1399–1404.

[6] P.A. Rota, M.S. Oberste, S.S. Monroe, W.A. Nix, R. Campagnoli, J.P. Icenogle, S. Penaranda, B. Bankamp, K. Maher, M.H. Chen, S. Tong, A. Tamin, L. Lowe, M. Frace, J.L. DeRisi, Q. Chen, D. Wang, D.D. Erdman, T.C. Peret, C. Burns, T.G. Ksiazek, P.E. Rollin, A. Sanchez, S. Liffick, B. Holloway, J. Limor, K. McCaustland, M. Olsen-Rasmussen, R. Fouchier, S. Gunther, A.D. Osterhaus, C. Drosten, M.A. Pallansch, L.J. Anderson, W.J. Bellini, Characterization of a novel coronavirus associated with severe acute respiratory syndrome, Science 300 (2003) 1394–1399.

[7] Z. Luo, A.M. Matthews, S.R. Weiss, Amino acid substitutions within the leucine zipper domain of the murine coronavirus spike protein cause defects in oligomerization and the ability to induce cell-to-cell fusion, J. Virol. 73 (1999) 8152–8159.

[8] B.J. Bosch, R. van der Zee, C.A. de Haan, P.J. Rottier, The coronavirus spike protein is a class I virus fusion protein: structural and functional characterization of the fusion core complex, J. Virol. 77 (2003) 8801–8811.

[9] D. Rapaport, M. Ovadia, Y. Shai, A synthetic peptide corresponding to a conserved heptad repeat domain is a potent inhibitor of Sendai virus-cell fusion: an emerging similarity with functional domains of other viruses, EMBO J. 14 (1995) 5524–5531.

[10] A. Fiser, A. Sali, Modeller: generation and refinement of homology-based protein structure models, Methods Enzymol. 374 (2003) 461–491.

[11] R.A. Laskowski, D.S. Moss, J.M. Thornton, Main-chain bond lengths and bond angles in protein structures, J. Mol. Biol. 231 (1993) 1049–1067.

[12] J.U. Bowie, R. Luthy, D. Eisenberg, A method to identify protein sequences that fold into a known three-dimensional structure, Science 253 (1991) 164–170.

[13] N. Sreerama, R.W. Woody, Estimation of protein secondary structure from circular dichroism spectra: comparison of CONTIN, SELCON, and CDSSTR methods with an expanded reference set, Anal. Biochem. 287 (2000) 252–260.

[14] B.W. Matthews, Solvent content of protein crystals, J. Mol. Biol. 33 (1968) 491–497.

[15] W. Li, M.J. Moore, N. Vasilieva, J. Sui, S.K. Wong, M.A. Berne, M. Somasundaran, J.L. Sullivan, K. Luzuriaga, T.C. Greenough, H. Choe, M. Farzan, Angiotensin-converting enzyme 2 is a functional receptor for the SARS coronavirus, Nature 426 (2003) 450–454.

[16] S.K. Wong, W. Li, M.J. Moore, H. Choe, M. Farzan, A 193-amino acid fragment of the SARS coronavirus S protein efficiently binds angiotensin-converting enzyme 2, J. Biol. Chem. 279 (2004) 3197–3201.

[17] Y. Xu, Y. Liu, Z. Lou, L. Qin, X. Li, Z. Bai, H. Pang, P. Tien, G.F. Gao, Z. Rao, Structural basis for coronavirus-mediated membrane fusion. Crystal structure of mouse hepatitis virus spike protein fusion core, J. Biol. Chem. 279 (2004) 30514–30522.

[18] K.A. Baker, R.E. Dutch, R.A. Lamb, T.S. Jardetzky, Structural basis for paramyxovirus-mediated membrane fusion, Mol. Cell 3 (1999) 309–319.

[19] X. Zhao, M. Singh, V.N. Malashkevich, P.S. Kim, Structural characterization of the human respiratory syncytial virus fusion protein core, Proc. Natl. Acad. Sci. USA 97 (2000) 14172–14177.